Engler *et al.*
Journal of Engineering and Applied Science (2024) 71:35
https://doi.org/10.1186/s44147-023-00331-4

Journal of Engineering and Applied Science

RESEARCH Open Access

Improving the surface quality of AlMgSi1 alloy with the selection of the appropriate vibration grinding stones

Carsten Engler[1*], Anthimos Georgiadis[1], Dirk Lange[1] and Nicolas Meier[1]

*Correspondence: Carsten.Engler@stud.leuphana.de

[1] Institute for Production Technology and Systems (IPTS), Universitätsallee 1, 21335 Lüneburg, Germany

Abstract

The number and variety of paints and coating systems in the automotive industry have increased in recent years. However, the basic requirement for the quality of the paints still depends on the surfaces on which they are applied. This applies not only to the large body parts but also to all components that are integrated.

There are many surface treatment processes and techniques that are used as an additional process step, such as pickling for a chemical surface treatment or blasting for a mechanical surface treatment.

The present work investigates a method for optimizing the surface before painting, using the membrane cup of the ultrasonic sensor as an example for AlMgSi1 alloy, without implementing additional process steps.

First, all process steps influencing the surface quality for the production of a membrane cup were considered for optimization. Then, based on a backward process chain analysis, vibratory grinding for deburring of the membrane cup was determined as the process step to be optimized. For the optimization of the vibratory grinding, experiments with two different grindstones were performed. For the characterization of the surface quality, the roughness parameters Rz and Ra were measured with a confocal laser scanning microscope and analyzed in order to determine the optimal process conditions.

The experiments showed that the surface roughness can be significantly improved using dedicated process parameters and taking into account the geometry of the vibratory grinding stones. Moreover, different surface qualities can be achieved at different areas on the workpiece, this new approach provides a solution for surface optimization in various areas of the workpiece without additional process steps and costs.

Keywords: Vibration grinding, Surface optimization, Roughness, Confocal laser scanning microscope, Six sigma

Introduction

The number and variety of paints and coating systems in the automotive industry have increased in recent years. However, the basic requirement for the quality of the paints still depends on the surfaces on which they are applied. This applies not only to the large

body parts but also to all components that are integrated.

One customer requirement, not only in the automotive industry, is the selection of optimal processes and process parameters to "improve the productivity and high quality with minimum cost" [1].

Process optimization to improve part quality is a well-known topic in science and industry. The optimization of processing parameters using soft computing techniques [1] is a good approach, reducing the cost of experiments with the help of software support. A model-based approach for process parameter optimization is well described in [2]. Using different materials as part of a process optimization is stated in [3]. In [4], an approach is described at an early stage for designers.

In contrast to all these approaches, this work involves a process chain with an influence on the surface quality. The incentive and motivation for this work is to analyze the process chain in order to first find a method for optimizing the surface before painting without carrying out additional process steps in order to achieve the customer requirement of "minimum costs" and to create an ideal basis for the painting process.

Research on surface optimization and analysis is also ongoing in science and industry, as shown, for example, in the papers by [5–9].

Surface coating, applied in [5, 6], is one opportunity for surface optimization. Advantageously, depending on the requirement, a high variety of surface qualities can be realized. Introducing a coating process would mean an additional process step for this work, which would lead to higher effort and costs. The use of friction for surface modification is discussed in [7] and is already present in the current production processes of the membrane pot, with the advantage that no additional process steps need to be established. The water jet treatment discussed in [8] as a surface optimization is considered a promising approach, but it would lead to an additional process step in this work and is therefore not the first choice. In [9], vibratory grinding is considered a process for deburring the produced part.

In line with the existing process chain for the membrane cup, deburring with vibratory grinding is already in place.

For this reason, special attention is paid to this step in the process chain analysis. The new approach and motivation for this work is the optimization of the vibratory grinding process in order to use this method not only for deburring but also for surface optimization. In addition to this motivation, the geometry of the vibratory grinding stones is also of great interest in order to achieve a surface finish exclusively in a specific area of the workpiece, which is also a new approach to optimize the vibratory grinding process.

The present work provides a further and essential contribution, both in process optimization and in the optimization or modification of surfaces. An optimization of the surface quality, or rather the surface properties, by adapting already existing processes is of major industrial interest since this information can serve a verity of purposes in the industry and results in lower risks and costs compared to the introduction or definition of additional processes.

The optimization of paint surfaces is a well-known and as yet an unsolved problem in science and industry. This work offers further optimization potential in an experimental investigation of the vibratory grinding process and is therefore of particular importance as it helps to investigate a method for optimizing the surface before painting. This study

takes into account both industrial and scientific aspects at the same time. The industrial importance of this work is underlined by the selection of the research object. With the membrane cup of the ultrasonic sensor of the automotive industry, a representative component was chosen with which the central aspects of many sensors can be investigated and additionally make a contribution to the way to autonomous driving.

For a better overview, the results are presented in compact form. The results are interpreted and analyzed by means of statistical significance. A verification of the statistical significance is a Six-Sigma method. Six Sigma methods are well-known in quality management. In addition to the case study from [10], this paper provides an additional practical case study, applying Six Sigma methods.

The membrane pot and the associated processes influencing the surface quality are described in detail, as well as the measuring system used for the analyses. As measuring system, a confocal laser scanning microscope was engaged, that previously was examined for the suitability of its operational purposes. The approach of the examination is described in detail. The subsequent chapter presents and analyzes the results of this examination. The final chapter summarizes this work and provides an outlook on further optimization potential for surface quality.

Methods

Membrane pot, the applied part for the experiment

With the ultrasonic sensors in the automotive industry, various driving functions and driving situations will be assisted. For a better illustration, Fig. 1 constitutes two variants of the ultrasonic sensor from two different manufacturers.

An essential function of these sensors is perceived as assistance in parking with acoustic signals. To better explain the operation of the sensor and the membrane pot, the individual components are displayed in Fig. 2.

An ultrasonic sensor is composed of a plastic molded housing with integrated plug-in connector, an ultrasonic transducer (membrane pot, glued on the inner side with a piezo ceramic oscillator), and a printed circuit board with transmit- and electric evaluation [11].

The membrane pot, constituted in Figs. 3 and 4, is suitable as representative component for various reasons, the essential ones are listed below:

- Aluminum component (AlMgSi1)
- A multitude number of painting systems are used in the automotive industry

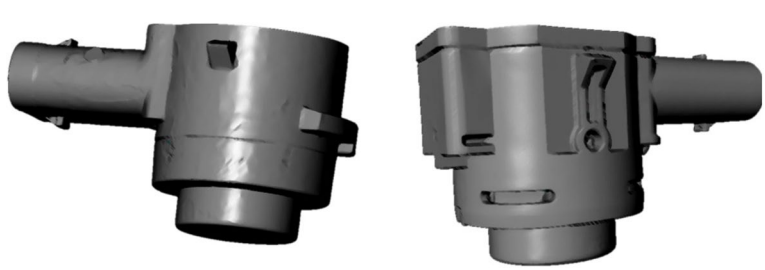

Fig. 1 Ultrasonic sensors of two manufacturers (own research)

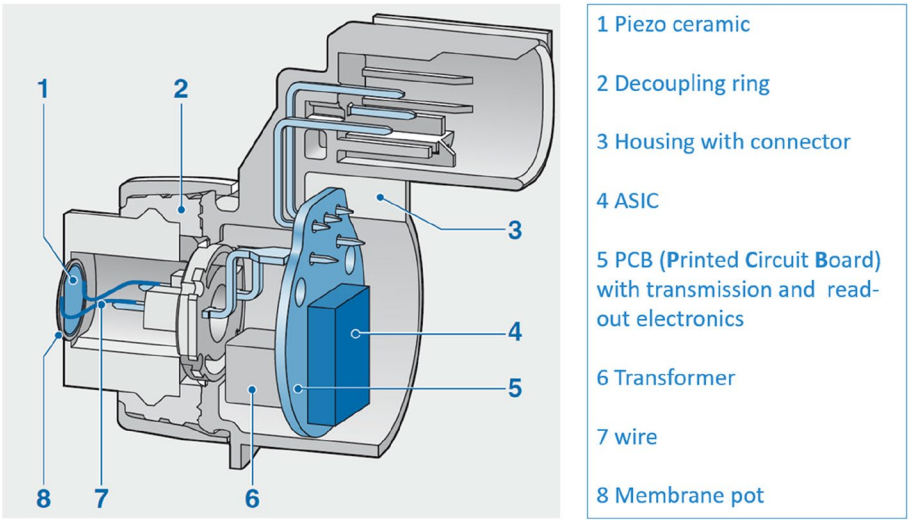

Fig. 2 Basic setup of an ultrasonic sensor in the automotive industry [11]

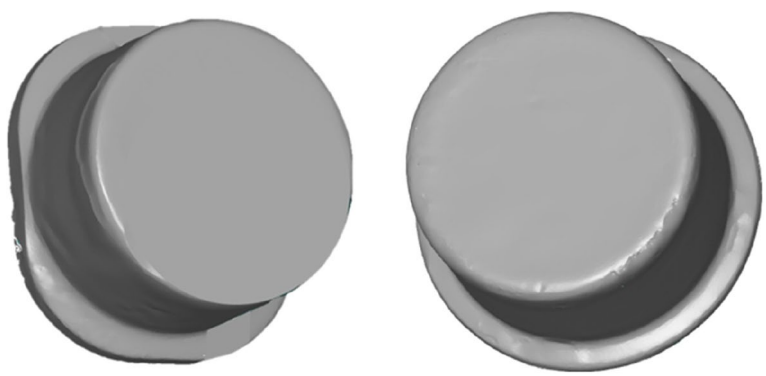

Fig. 3 Membrane pot exterior, painted in vehicle color (own research)

- The surface quality can be influenced by production processes
- Different surface qualities are required for the paint and for the glue

Aluminum, as a basic material in the industry, is painted in a variety of applications. The membrane pot is part of the ultrasonic sensor in the automotive industry, mounted in the front and/or rear bumpers. In accordance with the explanation of [11], the paintwork of the membrane pot is not essential for the function of the ultrasonic sensor. Paintwork of the membrane pot in vehicle color is a requirement of the automotive manufacturers, to facilitate a consistent optical color picture of the vehicle. Besides the functional requirements, a particular optical requirement exists for the membrane pot, thus the surface quality corresponds to a significant role. Improving the paint quality is of major industrial interest and motivation of this work.

Figure 3 shows the outside of two membrane pots from two different manufacturers to which the paint is applied.

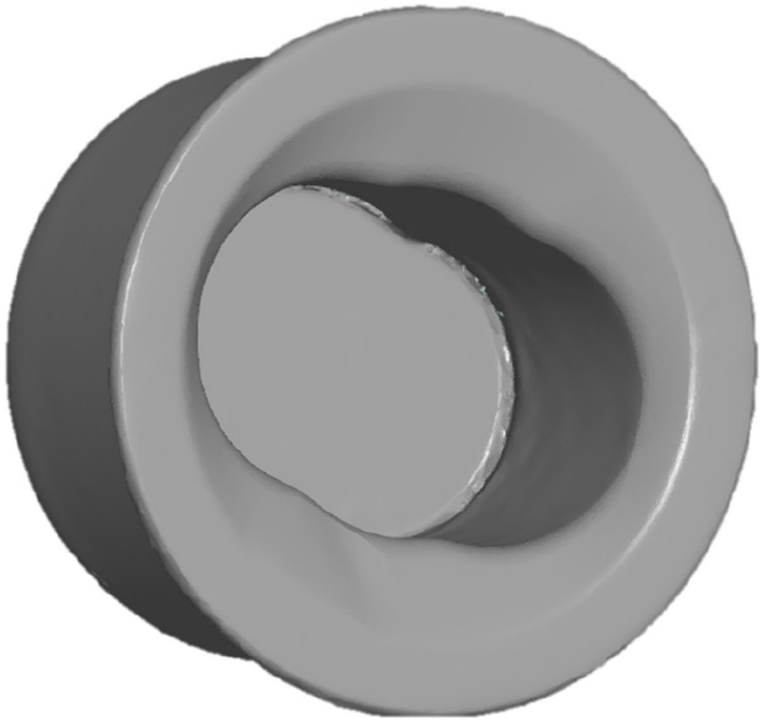

Fig. 4 Membrane pot interior, surface for piezo gluing (own research)

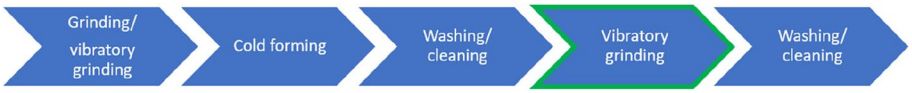

Fig. 5 Process steps with influence on surface quality (own research)

Figure 4 visualizes the inner side of the membrane pot. On the inner side, the piezo ceramic is glued.

Figures 3 and 4 demonstrate, in an ideal situation, two different surface qualities can be realized for the inner and outer sides of the membrane pot. A new approach and the motivation of this work is to find a solution for the optimization of the surfaces of different areas of the membrane pot by optimizing already existing manufacturing processes.

The surface quality of the outer side ought to be optimized for the lacquer in vehicle color. The inner side is for the gluing of the piezo element. An optimized surface for painting and a different surface quality for the gluing process require different surface qualities for the different areas of the membrane pot.

When considering the processes that affect surface quality, these requirements should be taken into account.

Vibratory grinding, the studied process

Having established an understanding of the membrane pot and its functions, Fig. 5 shows the main production processes affecting surface quality.

A backward process chain analysis was used to identify the optimization potential of the second vibratory finishing process, which is described and presented in this study.

Reverse straightening is recommended in this case because there are fewer subsequent processes that could affect the surface quality. To better explain the potential for improvement, the process chain shown in Fig. 5 is described in detail. The transformation of the workpiece at ambient temperature without external heating is characterized by cold forming. Besides this technical definition, a metallophysical for cold forming is presented as long as the transformation temperature of the workpiece is below its recrystallization temperature. Upsetting and extrusion are the main processes of cold forming [12].

Chipless forming is facilitated by reducing friction, e.g., by optimized sliding conditions, and by appropriate heat treatment:

1. For the sliding surface of the tool or rather the sheet surface with the application of a lubricant.
2. For the crystals of the forming material with heat treatment among the follow-up trains [13].

Following the execution of [13], the imperative shown in Fig. 5 is dedicated to washing and cleaning processes. Vibratory grinding is the second essential process step with the influence of the surface quality of the membrane cup. With vibratory grinding, two challenges can be solved in this study, the deburring and the surface optimization of the membrane cups. Deburring with vibratory grinding is well known in science and industry and well described in [9]. The new approach in this work is to optimize the vibratory grinding process not only for deburring but also for surface optimization. Another new feature is that the geometry and size of the vibratory finishing stones can be used to optimize only certain areas of the object.

According to standard DIN 8589–17, vibratory grinding belongs to the main group "cutting" or rather to the group "machining" with geometrically undefined cutting. According to the standard, sliding clamps are defined as machining that takes place in many loose abrasive bodies or abrasive materials and irregular relative movements between the workpieces. This results in chip removal. The geometry, size, and composition of the abrasive bodies matching to the proceeded workpieces [12].

Figure 6 schematically displays the rotary barrel finishing. The workpieces and working media are put into one drum. When the drum rotates at a certain speed, the workpieces and abrasive blocks in the drum are lifted with the rotation direction of the drum. In the lifting process, the workpieces and abrasive blocks located at the bottom of the drum are in a dynamic balance, and they remain relatively motionless. When the workpieces and abrasive blocks located at the top of the drum are lifted to a certain height, they will lose their balance and slide down. "Therefore, with the rotation of the drum, the workpieces and abrasive blocks in the drum roll over and over, which cause the collision, rolling, rubbing, and scoring among workpieces and abrasive blocks, and the finishing is implemented" [14].

"Rotary barrel finishing is one of the barrel finishing technologies at the earliest stage, and it is suitable for the finishing of small special-shaped parts" [9]. The approach in this work of optimizing the grinding process not only for finishing but rather for optimizing the surface quality of various areas, is new and of interest in science and industry.

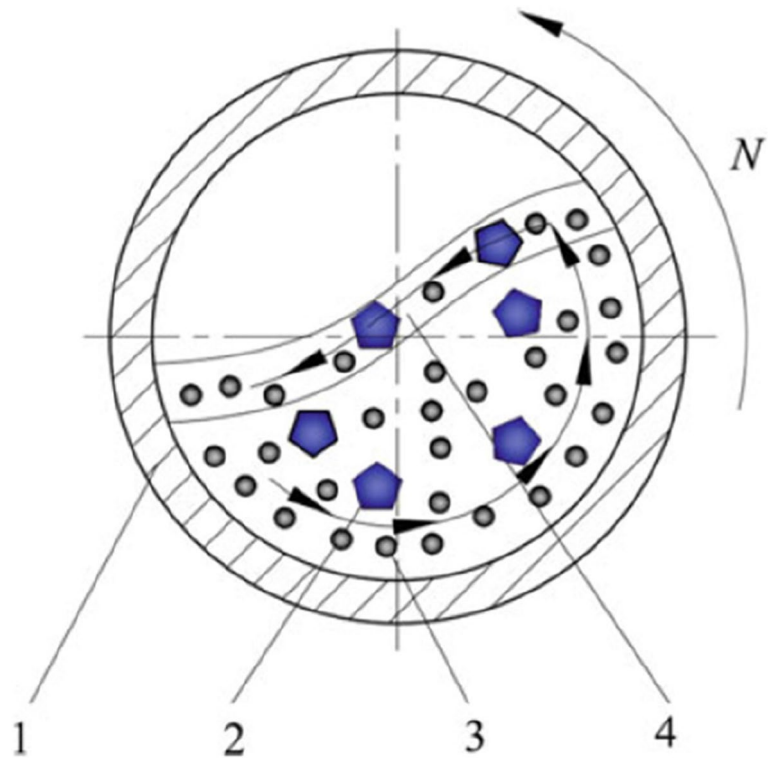

Fig. 6 Schematic of rotary barrel finishing. 1—drum; 2—workpieces; 3—working; medium; 4—sliding layer [14]

The proceeded workpieces, the abrasive bodies, and a liquid chemical medium (compound) are in a working tank. The desirable metal cutting occurs with an undefined relative movement between the abrasive bodies and the workpieces, evoked by a rotation, or vibration, as well as by a movement of the workpieces in a stationary filling of abrasive bodies. The selection of the appropriate grindstone depends primarily on the desired output. For a high material removal rate, and brief processing times, an abrasive chip type ought to be considered. Plastic-bonded grindstones are recommended for fine processing workpieces with true to gauge drills, tight tolerance fits or rather for the achievement of surfaces for electroplated coating [12]. The roughness of the surface is primarily determined through the selection of the grindstones. The larger the grindstone, the greater the grinding performance, the rougher the generated surface. Based on this information, the focus and trials were placed on the grinding stones instead of changing the process parameters for the rotary kiln. In this work, two different new synthetic resign grindstones are applied to examine the surface quality with regard to roughness. In addition to the material selection of the grinding stones, the geometry was also taken into account in order to fulfill the second goal of this work, namely not only to improve the surface quality but rather to offer a solution to create different areas of the object with different surface qualities. As a result, the vibratory finishing process has no influence on the surface of the inside and a separate area for separate surface optimization could be realized.

Table 1 Comparison of vibrating grindstones (own research out of the respective material data sheets)

Characteristic/grindstone	*A*	*B*
Specific weight [g/cm^3]	1.71	1.51
Design	Pyramid	Pyramid
Edge length [mm]	25	25
Carrier material	Plastic	Plastic
Manufacturing process	Molding	Molding
Additional manufacturing process	Curing/tempering	Curing/tempering

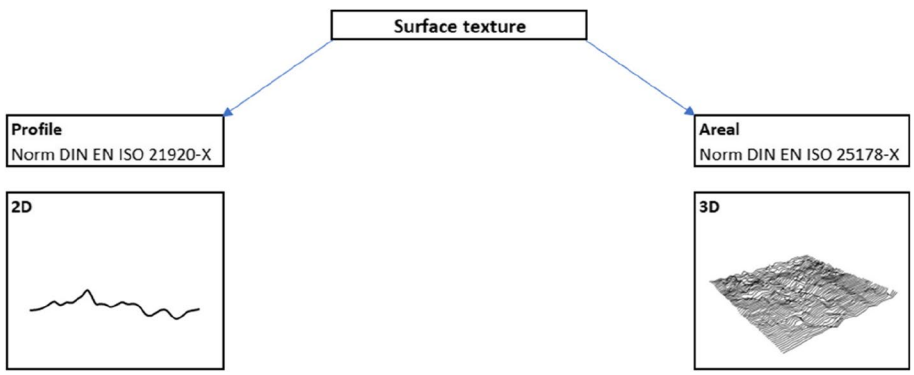

Fig. 7 Description of surface texture in standards (own research out of [16])

The aim was exclusively to change the surface of the outer area on which the paint was applied.

The following Table 1 compares the properties of the applied grinding stones.

Limitations of the grindstones are given in size, design, and material. These limitations must be taken into account for each application.

Roughness, the analyzed characteristic

To determine the surface quality or surface properties, various surface parameters can be analyzed. DIN Deutsches Institut für Normung e.V [15] defines the geometric parameters as waviness, roughness, and profile parameters. The surface finish of components can thus essentially be described by two standards, which are displayed in Fig. 7 for better understanding.

The selection of the profile roughness parameters or the area depends on the type of characterization of the surface properties. At the customer's request, the profile parameters Rz and Ra are examined in this work. This is designated as a profiled surface description. The roughness profile, also stated as R-profile, constitutes the basis for the evaluation of the R-characteristics [17, 18]. Parameters for the extensive surface finish are characterized in [16, 17]. DIN Deutsches Institut für Normung e.V [18, 19] defines the length of the measuring section for the evaluation according to roughness parameters. As a general rule, five individual measuring sections are applied as a basis for calculating the values of the parameter of the roughness profile. Figure 8 illustrates this relationship.

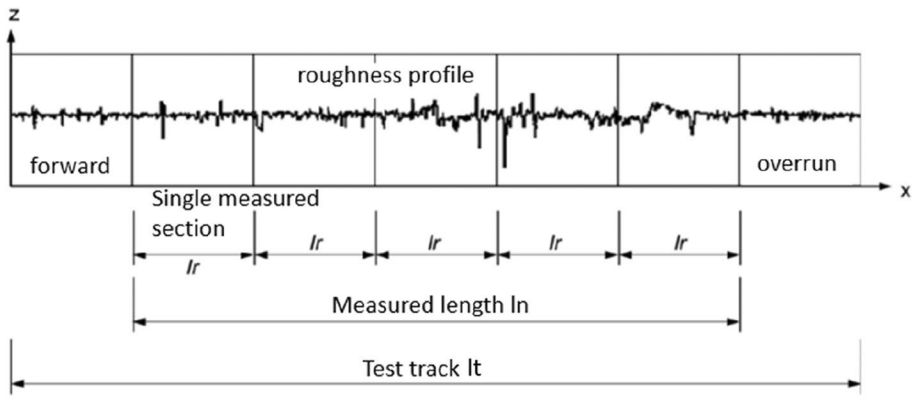

Fig. 8 Definitions of roughness profile [20]

According to [15], a measured distance ln is recorded and evaluated. Standard DIN EN ISO 21920–2 applies the term evaluation length le. Rz is determined on the basis of the single measuring distance, and Ra on the basis of the evaluation length. Le is the length in the direction of the x-axis, applied to determine the geometric structures. In Fig. 8, the procedure is described by means of the recording of the image. DIN Deutsches Institut für Normung e.V [21] advises for Rz values with upper tolerance limit in appendix B.2 an evaluation length le of 4 mm, for Ra values from appendix B.4 an evaluation length of 5 mm. According to Table 1 and 2 of [19], a single measuring distance lr of 0.8 mm and a measuring distance of 4 mm are advised, for both, the characteristic values Ra and Rz.

The stylus method is a frequently used method for determining roughness in the automotive industry and mechanical engineering [20]. This method is preferred by the customer. After initial trials with the stylus method and consultation with the customer, this method was discarded due to the visible change in the surface, which could lead to repeatable and reproducible problems, see Fig. 9. In alignment with the customer and a measuring device manufacturer, a confocal laser microscope was determined, which is explained in the next chapter.

Confocal laser microscopy, the applied measurement device

Since the stylus method did not allow repeatable and reproducible measurements, the focus of this work was set on an optical measuring instrument for evaluating surface quality. The experiments with white light interferometry were promising. The maximum working distance of 10 mm made measuring the inside of the membrane cup unfeasible, why it was not considered in this work. In addition to a confocal laser scanning microscope, a measuring device based on focus variations provided feasibility. The confocal laser scanning microscope was chosen due to the following main advantages:

- High precise measurements with 65,536 Gy scales
- Automated adjustment of the scanning area
- Microscope was easier to handle, also experienced by the customer
- Fast focus adjustment with automated focus recognition
- Lower investment costs

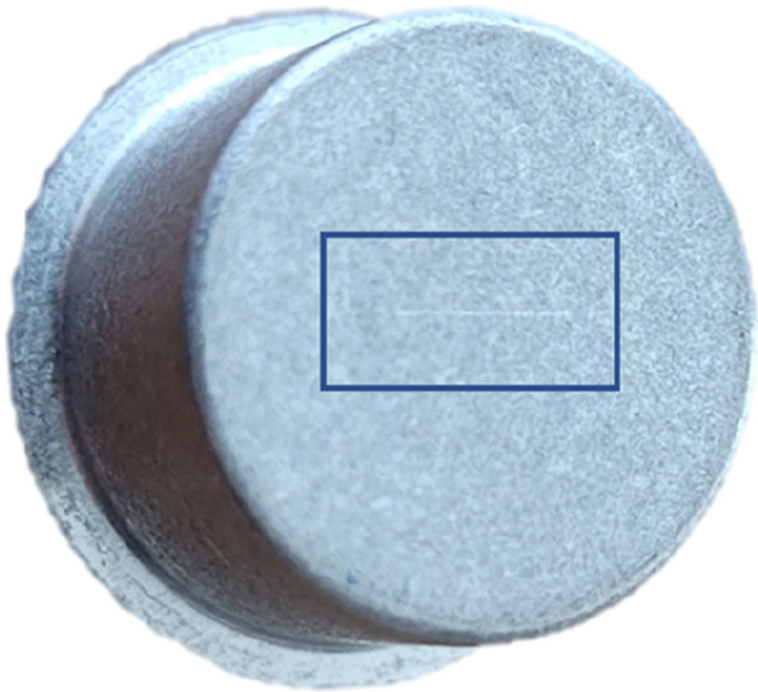

Fig. 9 Visible change in the membrane pot surface with the stylus method (own research)

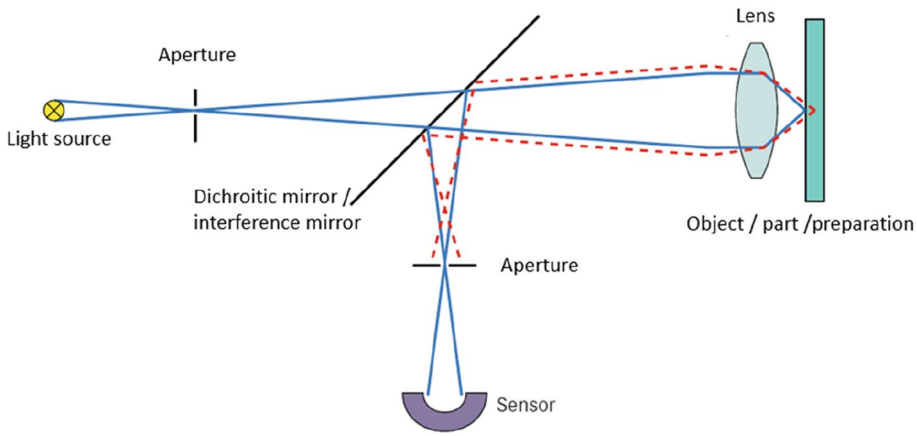

Fig. 10 Schematic representation of a confocal optical path [22]

With the application of a confocal laser scanning microscope, disturbing background information can be significantly reduced as one advantage of using this type of microscope. Confocal microscopic images are characterized by a significantly higher optical resolution and a stronger image contrast. When it comes to analyzing thick and highly scattering specimens such as a whole piece of tissue, the advantages of a confocal laser scanning microscope are appreciated [22]. The term "confocal" was established in 1977 by C. J. R. Sheppard. Confocal describes very precisely the optical setup, particularly the coincidence ("con") of the lighting, -and observation focal point ("focal") [23]. The basic setup of the confocal scanning microscope is visualized in Fig. 10.

Typical optical resolution values, obtained with a confocal laser scanning microscope, are approximately 200 nm lateral (x–y direction), and 500 nm axial (z-direction). The resolution limit depends on the numerical aperture, the applied objective lens, and the wavelength of the generated fluorescence. Modern confocal laser scanning microscopes apply lasers with different wavelengths for fluorescence stimulation. The laser light will focus on the preparation and lead over by means of a scanner mirror. The confocal laser scanning microscope helps quite excellently, as it optically cuts out only the sharp layer from the out-of-focus area. Therefore, it is also occasionally designated as "layer section microscope", or "optical microtome" [23]. Modern confocal laser scanning microscopes enable far more than simply fading of fluorescent fuzziness. Confocal laser scanning microscopes feature high-precision tuning of temporal and spatial laser intensities, the ability to perform spectral emission analysis, and synchronous imaging of cell structures with different lasers. Thus, confocal laser scanning microscopes are increasingly finding their application in analytical image processing systems [22]. There are variants with dielectric layers, and such with thin metallic films. Interference filters can be designed for any spectral transmission characteristic and allow steep edges in the transmission spectrum [24]. The measurement, assessment, and characterization of surfaces is a much-discussed topic in industry and science [8, 25]. In [26], "optical microscopy", "optical profilometry", and "X-ray computed tomography" are presented as three measurement devices for surface evaluation. The confocal laser microscope used in this analysis allows both areal and profile evaluation of the topography and is also unused in [27]. The laser scanning microscope, applied for this execution, owns a resolution of 1 nm, and operates with a telecentric objective lens to eliminate aberrations.

Such systems are often applied in metrology since the apparent image size does not change when the scanning distance is changed (within certain limits). A photomultiplier is applied as a laser receiving element, enabling a scanning frequency of 16 bits. Sixteen bits (2^{16}) acquisition implies a capturing in, 65,536 Gy levels. By means of this sensor, it is feasible to achieve high-resolution scanning. For better comprehensibility, the principle of this sensor is briefly illustrated. Figure 11 constitutes the basic design of this sensor.

A photomultiplier tube consists of a photocathode, an electron multiplier, and an anode, and is usually housed in an evacuated glass tube. When the photomultiplier tube starts, the incident light, which needs to be detected, passes through the input window.

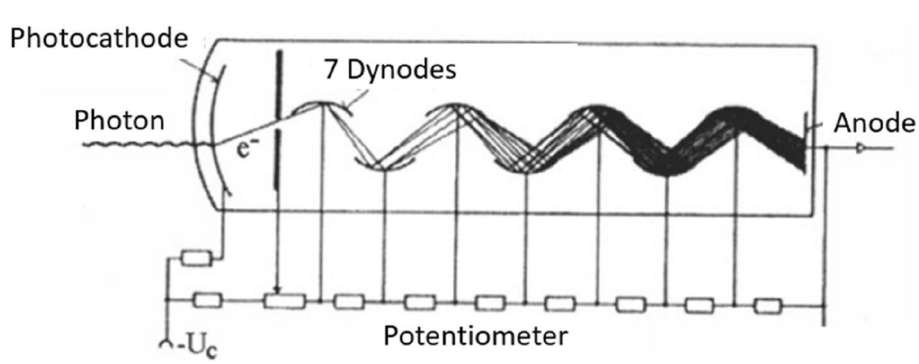

Fig. 11 Principle of the photomultiplier vacuum tube [28]

The electrons in the photocathode are emitted into the vacuum. Photoelectrons are focused by the focusing electrode onto the first dynode where they are multiplied by secondary electron emission. This process is repeated at each successive dynode. Finally, multiplied secondary electrons emitted from the last dynode are collected by the anode to form the anodic photocurrent. When the anodic photocurrent flows through the load resistance, a signal voltage is generated, which is used for detection [29]. Various arrangements of electrodes for focusing and accelerating the photoelectrons are applied in industrially manufactured photomultipliers. For an arrangement of 14 such successive dynodes with approx. 150–200 V potential difference between each dynode, a multiplication of the electron number (amplification) of 10^8 can be accomplished [28].

Table 2 constitutes the parameters, that can be imaged with the applied focal laser scanning microscope.

Six sigma method

Six Sigma is a process-orientated approach and "aims for virtually error-free business performance" [30]. "Six Sigma is a rigorous, focused, and highly effective implementation of proven quality principles and techniques" [30]. "As a data-driven approach, Six Sigma projects focus on how to reduce variation, waste, defects, and defective products or services" [31]. The aim of this work is an improvement of the surface quality, which means reducing the variation and defects in order to produce a zero-failure process. Six Sigma offers methods to achieve this goal. Six Sigma uses statistical methods to prove the effectiveness of the measures. These statistical methods are known to the companies and are applied by them. The application of Six Sigma methods represents the industrial focus of this work. The focus on the use of Six Sigma to improve the quality of processes corresponds exactly to the aim of this work, which is why Six Sigma was selected as a suitable method. According to Six Sigma, only statistically verified measures may be introduced.

A suitable method from the Six Sigma toolbox for comparing the results of the two different grindstones originates from descriptive statistics, which compares the mean value. The arithmetic mean can display metrological differences in these examinations. The results, displayed in Table 3 and 4, correlate both materials with its arithmetic means $\bar{x}$. For this appraisal, random samples produced with two different grindstones were considered. In this method, the values are tested for statistical significance using a *t*-test. For statistical tests, see as well [32, 33]. A difference can be determined whenever

Table 2 Representative surface roughness parameters (own research out of [16, 18])

Parameter	Designation
Spc	Arithmetic mean value of peak curvature
Sa	Mean arithmetic height of the scale-limited surface area
RSm	Mean spacing of the profile elements
Ra	Arithmetic mean value of the height
Sdr	Developed transition area ratio of a scale-limited surface
Str	Aspect ratio of the surface texture
Sz	Maximum height of the scale-limited surface
Rz	Maximum height

Table 3 Results Rz for vibrating grind stone A and B (own research)

Part	Rz value in [µm] with grindstone A	Rz value in [µm] with grindstone B
1	7.208	3.425
2	8.723	4.089
2	7.180	3.779
3	6.955	4.407
5	7.043	3.516
6	7.016	2.771
7	7.533	3.195
8	9.085	2.997
9	7.176	3.604
10	7.243	3.779
Mean value	7.516	3.556

Table 4 Results Ra for vibrating grind stones A and B (own research)

Part	Ra value in [µm] with grindstone A	Ra Wert in [µm] with grindstone B
1	1.044	0.370
2	1.499	0.415
2	1.205	0.401
3	1.149	0.447
5	1.241	0.372
6	1.289	0.312
7	1.195	0.379
8	1.376	0.353
9	1.114	0.474
10	1.109	0.442
Mean value	1,222	0,397

two random samples with their mean values are compared. The purpose of these test procedures is to indicate whether the observed difference is random or statistically significant. A significant difference means that the results of random scattering are doubtful. According to [34], three steps must be considered:

1. Calculation of the difference $\overline{d}$ of both random samples. Difference $\overline{d}$ means an estimate of true difference δ.
2. Calculation of the confidence level for the difference (with the same quantity for both random samples)
3. Interpretation of the results.

In this context, the confidence level is understood as:

> Due to the random dispersion of the sample values, the mean value of the sample will not completely match the mean value of the population. Thus, it is necessary to indicate an interval for the estimated parameter, the parameter of the population is within this interval with a determined probability. This interval is named confidence level or confidence interval [34].

Results and discussion

For the execution of both experiments, the same quantity of membrane pots was granted into the work vessel, subsequently, the operation was executed with the identical setting of the machine, with respectively the different grindstones, constituted in Table 1. Vibratory grinding produces primarily the deburring of the components. Hence, deburring is the precondition for both deployed grindstones. This precondition was visually checked for both grindstones with positive results.

These suggestions of standards 21,920 and 4288 were considered in this examination. The settings of the confocal laser scanning microscope were reviewed and determined with the manufacturer. A × 20 magnification was selected for the membrane pot. As a result of the manufacturer's setting recommendations, individual measuring distances of > 0.6 mm could be realized. From each image, 21 sensing distances were generated. This results in a measuring distance ln or an evaluation length le of more than 12 mm (21 × 0.6 mm). A confocal microscope has some limitations and leads to compromises. The higher the resolution, the higher the magnification, the smaller the image. Standard DIN EN ISO 4288 requires a single measuring distance lr of 0.8 mm and a measuring distance of 5 mm, which is not possible at high magnification. The software can merge many small images into a large one, but this leads to a longer processing time. The above parameter settings are the compromise discussed with the measuring device manufacturer and approved by the customer.

Figure 12 shows the measurement strategy resulting from the above-mentioned compromise. A surface topographic image of the outside of the membrane pot was established. In this sector, 21 sensing distances were defined. Each blue line represents a profile distance lt. All 21 scanning distances, defining the measuring distance ln, or the evaluation length le. The dimension of the recorded topographic area is constituted in Fig. 13. In this figure, the recorded heights are additionally represented by the adjacent color palette.

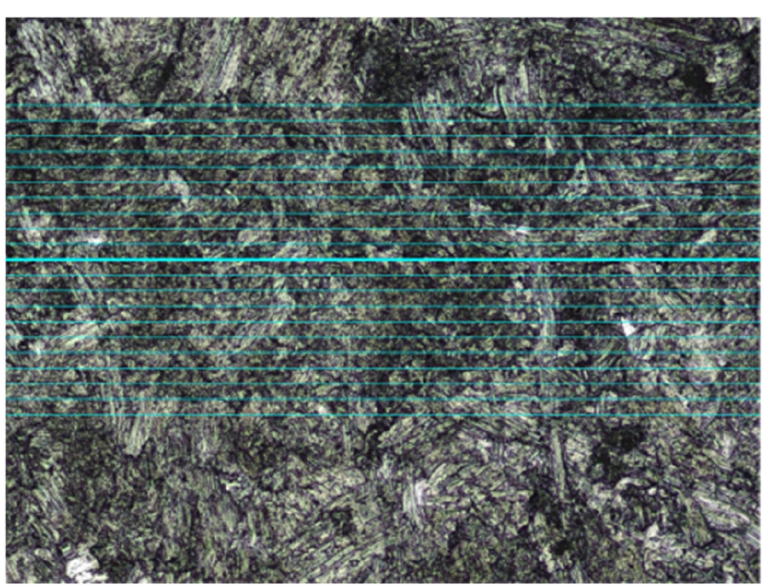

Fig. 12 Recording of the surface topography of the surface of a membrane pot (own research)

Figure 13 provides the limitations of the image with a × 20 magnification in the *x* and *y* direction. Both distances 0.71 mm in *x* direction and 0,53 mm in *y* direction do not fulfill the length of the standard DIN EN ISO 4288.

Figure 14 displays the roughness profile of a scanning path; this results in the single measuring path lr. Respectively, the two yellow lines visualize the forward and overrun.

Tables 3 and 4 constitute the measurement results of the roughness values of the membrane pots with the different vibratory grinding processes and grindstones.

Comparing the mean values Rz of the grindstones B and A results in a factor of 0.47. Whether this factor is statistically significant is then examined by applying a *t*-test from the Six Sigma toolbox. Ten measured values were aligned with the customer for a first trial, but limits the statistical significance.

With comparing the mean values Ra of the grindstones B and A, the result is even a factor of 0.32. This factor is also examined with this Six Sigma method.

According to the "Six Sigma" approach, decisions should only be derived after examining statistical significance, and further examinations ought to apply to decisions. For this appraisal, random samples with two different grindstone materials are rotary barrel finished. Two mean values are compared for the characteristic Rz and

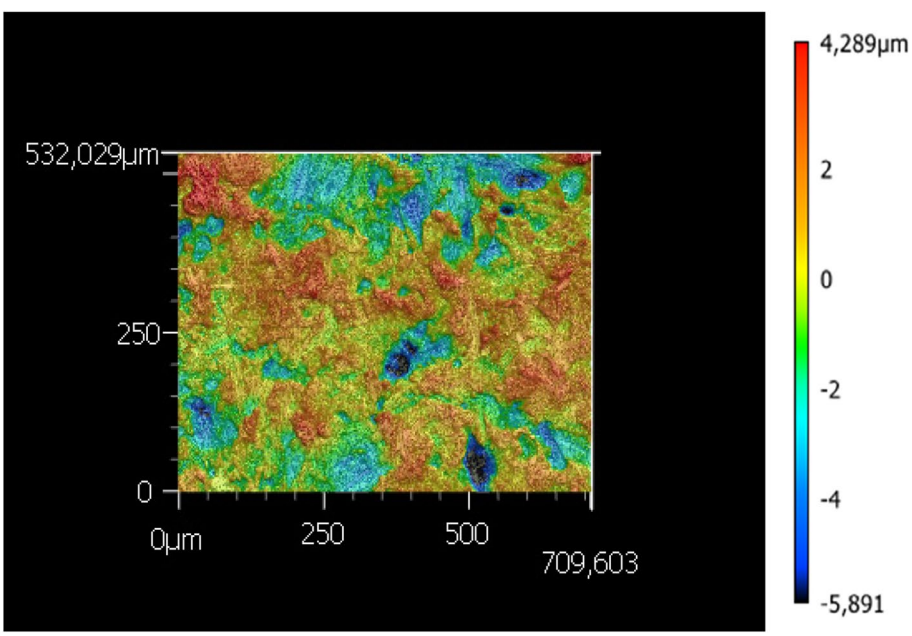

Fig. 13 Recorded topography area with a color scale of the height (own research)

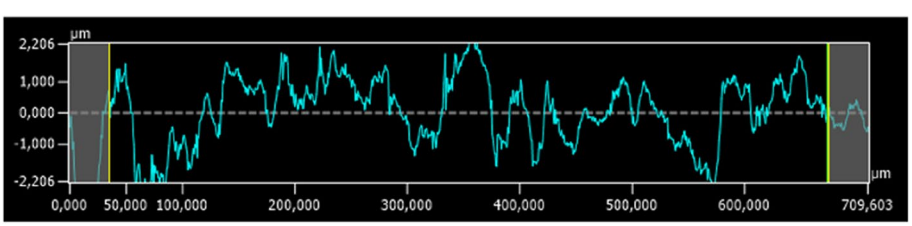

Fig. 14 Sensing distance lt und single measured section lr (own research)

Ra. In this method, a t-test was performed to test the values for statistical significance. A difference can be detected whenever two samples or their mean values are compared. The purpose of these test procedures is to indicate whether the observed difference is random or statistically significant. A significant difference means the results are doubtful from the random scatter. According to [34], three steps must be considered:

1. Calculation of the difference $\bar{d}_{Rz}$, and $\bar{d}_{Ra}$ of both random samples mean values for characteristics difference amounts to 3.960 µm and 0.825 µm. The difference $R\bar{z}$ and $R\bar{a}$ means an estimate of the true difference.
2. Calculation of the confidence level for the difference (with the same quantity for both random samples) [34]

$$\bar{d} - t^{*}s_{\bar{d}} \leq \delta \leq \bar{d} + *s_{\bar{d}};\ s_{\bar{d}} = \sqrt{\frac{2}{n}} * s^{2};\ \text{the standard deviation of the effect} \tag{1}$$

$$s^{2} = \frac{s1^{2} + s2^{2}}{2};\ \text{mean} - \text{variance of the single values} \tag{2}$$

<u>for Rz:</u> $s = 0{,}900$; $s_{\bar{d}} = 0.403$

$$N = 2 * n = 20;\ \text{the total amount of the test results} \tag{3}$$

$$f = 2 * (n - 1) = N - 2 = 18;\ \text{variances} \tag{4}$$

$t_{f=18.1\text{-}\alpha/2\,=97.5\%} = 2.101$, out of table *t*-distribution
3.960 µm – 2.101*0.403 ≤ δ ≤ 3.960 µm – 2.101 * 0.403; 3.114 µm ≤ δ ≤ 4.806 µm
<u>For Ra</u>: $s = 0.103$; $s_{\bar{d}} = 0.046$
$N = 2*n = 20$; the total amount of the test results
$f = 2 * (n—1) = N - 2 = 18$; variances
$t_{f=18.1\text{-}\alpha/2\,=97.5\%} = 2.101$, out of table *t*-distribution
0.825 µm – 2.101 * 0.046 ≤ δ ≤ 0.825 µm – 2.101 * 0.046; 0.729 µm ≤ δ ≤ 0.922 µm

3. Interpretation of the results

The confidence level excludes 0; for this reason, a significant difference applies between both grindstones [34].

In this context, the confidence level is understood as the following:

> Due to the random dispersion of the sample values, the mean value of the sample will not completely match the mean value of the population. Thus, it is necessary to indicate an interval for the estimated parameter, the parameter of the population is within this interval with a determined probability. This interval is named confidence level or confidence interval [34]. Furthermore, the mean range will be constituted even as a hypothesis test. The null hypothesis H0 estimates the mean of both populations is equal [34].

$$\begin{aligned} &t_{\text{krit}} = \text{t}_{\text{f}=18.1-\alpha/2=97.5\%} = 2.101;\ \text{critical}\ t-\text{value} \\ &t_{\text{pr}} = \overline{\text{d}}_{\text{Rz}}/\text{s}\cdot_{\overline{\text{d}}} = 9.84;\ \text{test value} \\ &t_{\text{pr}} = \overline{\text{d}}_{\text{Ra}}/\text{s}\cdot_{\overline{\text{d}}} = 17.99;\ \text{test value} \end{aligned} \tag{5}$$

The test value is significantly larger than the critical t-value; thus, the null hypothesis H0 must be rejected. For characteristic Rz and Ra, the two different grindstones are distinguished significantly. Thus, the goal of improved quality of the outer surface for the painting process could be achieved from a statistical point of view.

The exclusive consideration of statistics is a clear limiting factor for the Six Sigma method. The aim of this work is to improve the surface quality of paints. For example, if the statistical significance is not given, but the color result is better, the improvement should be implemented. The result of the coating can only be checked visually, so it is not sufficient to consider only the statistical result of the Six Sigma method.

In this study, technical relevance was used to overcome the limitations of the Six Sigma method. A measurable difference between $\overline{\text{d}}$Rz and $\overline{\text{d}}$Ra of 3.960 µm and 0.825 µm, with initial mean values of 7.516 µm for Rz and 1.222 µm for Ra, clearly represents technically relevant differences that are also visually reflected in the painting results.

All results were manually calculated and verified through the statistic software "Minitab".

Conclusions

The motivation of this work, to improve the surface quality through process optimization instead of implementing additional process steps in order to achieve a solution without major cost consequences, could be realized with the following steps:

1. Defining current processes with the influence of the surface quality.
2. Using a backward process chain analysis, the vibratory grinding process was identified as the process with which an improvement in surface quality can be achieved without having to introduce additional process steps.
3. A further optimization was achieved by taking into account the geometric properties of the grinding stones. This enables surface optimization in certain areas of the membrane pot. This is particularly important as the outer surface of the membrane pot is painted and a piezo element is glued to the inner surface. In this way, the surface of both areas can be optimized for the respective application.
4. Use of a confocal laser scanning microscope instead of the stylus method to avoid surface changes for reproducibility and repeatability.
5. The aim of improving the surface quality by selecting suitable vibratory finishing stones was evaluated using the roughness parameters Rz and Ra. The results illustrate the statistical significance, as the Six Sigma method, and its technical relevance.

Limitations were identified in:

1. The Size, design, and material of the grindstones. These restrictions must be taken into account for every application.

2. The stylus method was not feasible in this work due to the surface change caused by the needle used. The confocal laser scanning microscope has no influence on the surface, but certain limitations to meet the standard.
3. Evaluation with Six Sigma methods also has some limitations as it relies only on statistics, which should not be the only evaluation method, therefore technical relevance was applied in this work.

This approach can serve as a basis for future tests or a DoE (Design of Experiment) to further improve the surface quality. In addition to further attempts to optimize the outside of the membrane pot, an attempt can now also be made to optimize the inside. This approach can also be transferred to other applications, products, or processes. However, the limitations must be taken into account.

Abbreviations

Spc	Arithmetic mean value of peak curvature
Sa	Mean arithmetic height of the scale-limited surface area
RSm	Mean spacing of the profile elements
Ra	Arithmetic mean value of the height
Sdr	Developed transition area ratio of a scale-limited surface
Str	Aspect ratio of the surface texture
Sz	Maximum height of the scale-limited surface
Rz	Maximum height
lr	Single length
ln	Measured length
lt	Length test track
le	Evaluation lenght
DoE	Design of experiments

Acknowledgements
Not applicable.

Authors' contributions
CE: conceptualization, methodology, experimentation, measurement, data analysis, and writing. AG: conceptualization, Data analysis, validation, supervision, and review. DL: methodology, validation, supervision, and review. NM: validation and review. All authors have read and approved the final manuscript.

Funding
No funding was received for conducting this study.

Availability of data and materials
The datasets used and/or analyzed during the current study are available from the corresponding author on reasonable request.

Declarations

Competing interests
The authors declare that they have no competing interests.

Received: 25 September 2023 Accepted: 4 December 2023
Published online: 07 February 2024

References

1. El Hossainy TM, Zeyada Y, Abdelkawy A (2023) Machining process parameters optimization using soft computing technique. J Eng Appl Sci 70(1):1–3. https://doi.org/10.1186/s44147-023-00174-z
2. Lange A, Müller D, Kirsch B, Aurich JC (2022) Numerical analysis of process-tool-interactions in micro milling. Proc CIRP 108:299–304. https://doi.org/10.1016/j.procir.2022.03.051
3. Shiek J, Sairam J, Mouda PA (2023) Parameter optimization in the enhancement of MRR of titanium alloy using newer mixing method in PMEDM process. J Eng Appl Sci 70(1):1–6. https://doi.org/10.1186/s44147-023-00230-8
4. Swelem S, Fahmy A, Ellafy H (2022) Optimization of cold-formed lipped C-section under bending using prediction equations as objective functions. J Eng Appl Sci 69(1):1–3. https://doi.org/10.1186/s44147-022-00106-3

5. Aurich JC, Kieren-Ehses S, Mayer T, Bohley M, Kirsch B (2022) An investigation of the influence of the coating on the tool lifetime and surface quality for ultra-small micro end mills with different diameters. CIRP J Manuf Sci Technol 37:92–102. https://doi.org/10.1016/j.cirpj.2022.01.004
6. Chaharmahali R, Fattah-alhosseini A, Nouri M, Babaei K (2021) Improving surface characteristics of PEO coatings of Mg and its alloys with zirconia nanoparticles: a review. Appl Surf Sci Adv 6:100131. https://doi.org/10.1016/j.apsadv.2021.100131
7. Manroo SA, Khan NZ, Ahmad B (2022) Study on surface modification and fabrication of surface composites of magnesium alloys by friction stir processing: a review. J Eng Appl Sci 69(1):1–23. https://doi.org/10.1186/s44147-022-00073-9
8. Thakur PM, Raut DN (2023) Experimental investigation on surface topography in submerged abrasive waterjet cutting of Ti6Al4V. Adv Industr Manufact Eng 6:100113. https://doi.org/10.1016/j.aime.2023.100113
9. Boschetto A, Ruggiero A, Veniali F (2007) Deburring of sheet metal by barrel finishing. Key Eng Mater 344:193–200. https://doi.org/10.4028/www.scientific.net/KEM.344.193
10. Rath S, Agrawal R (2023) Prediction of novel operating parameters using Six Sigma: a study in the steel making process. Qual Manag J 30(3):187–201. https://doi.org/10.1080/10686967.2023.2211284
11. Reif K (2012) Sensoren im Kraftfahrzeug [Sensors in motor vehicles], (2., ergänzte Auflage). Springer Science+Business Media
12. Klocke F (2018) Zerspanung mit geometrisch unbestimmter Schneide [Machining with geometrically indeterminate cutting edge]. (6. Aufl.). VDI-Buch: Bd. 2. Springer Vieweg. http://www.springer.com/
13. Hellwig W (2006) Spanlose Fertigung: Stanzen. Grundlagen für die Produktion einfacher und komplexer Präzisions-Stanzteile ; mit 48 Tabellen [Chipless manufacturing: stamping. Fundamentals for the production of simple and complex precision stampings ; with 48 tables]. (8., aktualisierte und erg. Aufl.). Wiesbaden (Viewegs Fachbücher der Technik, 9783528740429)
14. Yang S, Li W (2017) Surface finishing theory and new technology. Berlin, Heidelberg, Springer Berlin Heidelberg. Online available: http://nbn-resolving.org/urn:nbn:de:bsz:31-epflicht-1516477.
15. DIN Deutsches Institut für Normung e.V (2010) DIN EN ISO 4287. Geometrische Produktspezifikation (GPS) – Oberflächenbeschaffenheit: Tastschnittverfahren – Benennung, Definitionen und Kenngrößen der Oberflächenbeschaffenheit [Geometrical Product Specification (GPS) – Surface texture: Profile method – Terms, definitions and surface texture parameters] (ISO 4287:1997 + Cor 1:1998 + Cor 2:2005 + Amd 1:2009). Berlin, DIN Deutsches Institut für Normung e.V
16. DIN Deutsches Institut für Normung e.V (2010) DIN EN ISO 25178–6: Geometrische Produktspezifikation (GPS) - Oberflächenbeschaffenheit: Flächenhaft - Teil 6: Klassifizierung von Methoden zur Messung der Oberflächenbeschaffenheit [Geometrical Product Specification (GPS) – Surface texture: Areal – Part 6: Classification of methods for measuring surface texture]. (ISO 25178–6:2010); Deutsche Fassung EN ISO 25178–6:2010. Berlin, DIN Deutsches Institut für Normung e.V
17. Abdelkawy A (2022) Modelling of cutting force and surface roughness of ultrasonic-assisted drilling using artificial neural network. J Eng Appl Sci 69(1):50. https://doi.org/10.1186/s44147-022-00105-4
18. DIN Deutsches Institut für Normung e.V (2022) DIN EN ISO 21920-2: Geometrische Produktspezifikation (GPS) - Oberflächenbeschaffenheit: Profile – Teil 2: Begriffe und Kenngrößen für die Oberflächenbeschaffenheit [Geometrical Product Specification (GPS) – Surface texture: Profile - Part 2: Terms, definitions and surface texture parameters]. (ISO 21920-2:2021, korrigierte Fassung 2022-06); Deutsche Fassung EN ISO 21920-2:2022. Berlin, DIN Deutsches Institut für Normung e.V
19. DIN Deutsches Institut für Normung e.V (1998) DIN EN ISO 4288. Geometrische Produktspezifikation (GPS) – Oberflächenbeschaffenheit: Tastschnittverfahren – Regeln und Verfahren für die Beurteilung der Oberflächenbeschaffenheit [Geometrical Product Specification (GPS) – Surface texture: Profile method – Rules and procedures for the assessment of surface texture] (ISO 4288:1996). Berlin, DIN Deutsches Institut für Normung e.V
20. Conrad KJ (2021) Taschenbuch der Konstruktionstechnik [Pocketbook of construction technology]. 3., vollständig überarbeitete und erweiterte Auflage. München, Hanser (Hanser eLibrary)
21. DIN Deutsches Institut für Normung e.V (2022) DIN EN ISO 21920–3: Geometrische Produktspezifikation (GPS) - Oberflächenbeschaffenheit: Profile – Teil 3: Spezifikationsoperatoren [Geometrical Product Specification (GPS) – Surface texture: Profile – Part 3: Specification operators]. Deutsche Fassung EN ISO 21920–3:2022. Berlin, DIN Deutsches Institut für Normung e.V
22. Mulisch M, Welsch U, Aescht E (2015) Romeis mikroskopische technik [Romeis Microscopic Technology], 19th edn. Springer Spektrum, Berlin, Heidelberg
23. Borlinghaus RT (2016) Konfokale Mikroskopie in Weiß. Optische Schnitte in allen Farben [Confocal microscopy in white. Optical sections in all colors]. Berlin, Heidelberg, Springer Spektrum. Online verfügbar unter http://www.springer.com/
24. Beyerer J, Puente LF, Frese C (2012) Automatische Sichtprüfung. Grundlagen, Methoden und Praxis der Bildgewinnung und Bildauswertung [Automatic visual inspection. Basics, methods and practice of image acquisition and image evaluation]. Berlin, Heidelberg, Springer Vieweg
25. Gradl PR, Cervone A, Gill E (2022) Surface texture characterization for thin-wall NASA HR-1 Fe–Ni–Cr alloy using laser powder directed energy deposition (LP-DED). Adv Industr Manufact Eng 4:100084. https://doi.org/10.1016/j.aime.2022.100084
26. Vidakis N, David C, Petousis M, Sagris D, Mountakis N, Moutsopoulou A (2022) The effect of six key process control parameters on the surface roughness, dimensional accuracy, and porosity in material extrusion 3D printing of polylactic acid: prediction models and optimization supported by robust design analysis. Adv Industr Manufact Eng 5:100104. https://doi.org/10.1016/j.aime.2022.100104
27. Singh M (2022) Development of a portable Universal Testing Machine (UTM) compatible with 3D laser-confocal microscope for thin materials. Adv Industr Manufact Eng 4:100069. https://doi.org/10.1016/j.aime.2022.100069
28. Kleinknecht K (2005) Detektoren für Teilchenstrahlung [Detectors for particle radiation], 4., überarb. Aufl. Wiesbaden, Teubner (Lehrbuch Physik)

29. Yan J (2019) Optical electronics: an introduction. De Gruyter graduate. Tsinghua University Press, de Gruyter
30. Pyzdek T, Keller P (2018) The six sigma handbook, 5th. McGraw-Hill Education
31. Pakdil F (2020) Six Sigma for students: a problem-solving methodology. Palgrave Macmillan. https://doi.org/10.1007/978-3-030-40709-4
32. Belouafa S, Habti F, Benhar S, Belafkih B, Tayane S, Hamdouch S, Bennamara A, Abourriche A (2017) Statistical tools and approaches to validate analytical methods: methodology and practical examples. Int J Metrol Qual Eng 8:9. https://doi.org/10.1051/ijmqe/2016030
33. Abdulwahab AE, Hubeatir KA, Imhan KI (2022) Optimization of PC micro-drilling using a continuous CO2 laser: an experimental and theoretical comparative study. J Eng Appl Sci 69(1):98. https://doi.org/10.1186/s44147-022-00151-y
34. Wappis J, Jung B (2016) Null-Fehler-Management Umsetzung von Six Sigma [Zero Defect Management Implementation of Six Sigma], 5., überarbeitete Auflage. Carl Hanser Verlag München Wien

Publisher's Note